

Field-Induced Magnetic and Structural Domain Alignment in PrO_2

C. H. Gardiner,^{1,*} A. T. Boothroyd,² M. J. McKelvy,³ G. J. McIntyre,⁴ and K. Prokeš⁵

¹*National Physical Laboratory, Queens Road, Teddington, Middlesex, TW11 0LW, UK*

²*Clarendon Laboratory, University of Oxford, Parks Road, Oxford, OX1 3PU, UK*

³*Center for Solid State Science, Arizona State University, Tempe, Arizona 85287-1704*

⁴*Institut Laue-Langevin, Boîte Postale 156, F-38042 Grenoble Cédex 9, France*

⁵*Hahn-Meitner Institut, SF-2, Glienicker Straße 100, D-14109 Berlin, Germany*

(Dated: May 23, 2019)

We present a neutron diffraction study of the magnetic structure of single crystal PrO_2 under applied fields of 0–6 T. As the field is increased, changes are observed in the magnetic Bragg intensities. These changes are found to be irreversible when the field is reduced, but the original intensities can be recovered by heating to $T > 122$ K, then re-cooling in zero field. The antiferromagnetic ordering temperature $T_N = 13.5$ K and the magnetic periodicity are unaffected by the applied field. We also report measurements of the magnetic susceptibility of single crystal PrO_2 under applied fields of 0–7 T. These show strong anisotropy, as well as an anomaly at $T = 122 \pm 2$ K which coincides with the temperature $T_D = 120 \pm 2$ K at which a structural distortion occurs. For fields applied along the $[100]$ direction the susceptibility increases irreversibly with field in the temperature range $T_N < T < T_D$. However, for fields along $[110]$ the susceptibility is independent of field in this range. We propose structural domain alignment, which strongly influences the formation of magnetic domains below T_N , as the mechanism behind these changes.

PACS numbers: 61.12.Ld, 75.25.+z, 75.30.Cr, 75.30.Kz

I. INTRODUCTION

In recent years there has been strong interest in Jahn-Teller and orbital phenomena in compounds containing localized $4f$ and $5f$ electrons. Among the simplest of these are the fluorite-structure actinide dioxides UO_2 and NpO_2 , which display complex ordered phases at low temperatures involving coupled electric and magnetic multipoles as well as (in the case of UO_2) a lattice distortion.^{1,2}

Unusual magnetic effects have also been observed in the lanthanide dioxide PrO_2 , which is isostructural with UO_2 and NpO_2 at room temperature and exhibits antiferromagnetic ordering below $T_N = 13.5$ K. Some years ago, PrO_2 was found to have an anomalously small ordered moment in the antiferromagnetic phase.³ More recently we discovered a broad continuum in the magnetic excitation spectrum probed by neutron inelastic scattering, which we ascribed to Jahn-Teller fluctuations involving the orbitally-degenerate $4f$ ground state and dynamic distortions of the lattice.⁴ In a separate neutron diffraction experiment⁵ we found evidence that the antiferromagnetic structure contains a component with twice the periodicity of the accepted magnetic structure, and we have recently reported further neutron diffraction studies⁶ which reveal an internal distortion of the fluorite structure below $T_D = 120 \pm 2$ K and a related distortion of the antiferromagnetic structure below T_N . These distortions result in a doubling of both the crystallographic and magnetic unit cells along one crystal axis. The magnetic structure is found to consist of two components: a primary component whose unit cell is the same as that of the undistorted crystal structure (referred to hereafter as the “type-I component”), and a secondary component with a smaller ordered moment, whose unit cell is the

same as that of the distorted structure (referred to hereafter as the “doubled component”).

In this paper we present neutron diffraction studies of the magnetic structure and measurements of the magnetic susceptibility of PrO_2 under applied magnetic fields of 0–7 T. The neutron diffraction experiments were designed to influence the alignment of symmetry-equivalent magnetic domains, in order to determine whether the type-I component of the magnetic structure was of the multi- \mathbf{q} type. These experiments produced unexpected results which suggest that the alignment of the magnetic domains is strongly influenced by a field-induced alignment of structural domains in the distorted phase below T_D .

II. MAGNETIC STRUCTURE UNDER APPLIED FIELD

As mentioned in the introduction, the magnetic structure of PrO_2 contains two components, the dominant one being the type-I antiferromagnetic structure which has a magnetic unit cell of the same dimensions as the unit cell of the undistorted fluorite crystallographic structure. The secondary (doubled) component of the magnetic structure is described in detail elsewhere.⁶ There are three possible type-I spin arrangements consistent with existing neutron diffraction data. These are the transverse multi- \mathbf{q} structures shown in Fig. 1. Longitudinal structures are ruled out by comparison of their magnetic structure factors with the measured Bragg intensities. Neutron diffraction measurements in zero field cannot distinguish between these three structures because they give rise to identical magnetic structure fac-

tors when averaged over symmetry-equivalent magnetic domains. One of the aims of the experiments described here was to influence the populations of the domains by cooling through T_N in a magnetic field, and hence to distinguish between the three structures.

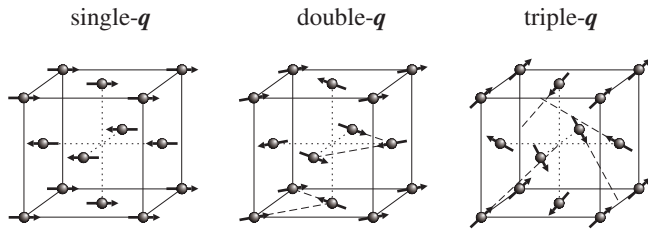


FIG. 1: Transverse multi- q magnetic structures for PrO_2 . The spheres are the Pr ions (the O ions are not shown in this diagram).

A. Experimental Details

Two neutron diffraction experiments were performed using the same crystal in different orientations with respect to the magnetic field. The first experiment was performed on the E4 double-axis single crystal diffractometer at the Berlin Neutron Scattering Centre at the Hahn-Meitner Institute. A flat pyrolytic graphite (002) monochromator was used in combination with a graphite filter. $40'$ collimators were placed before and after the monochromator, but there was no collimation between the sample and the detector. A square aperture of 10×10 mm was placed before the detector. The incident neutron wavelength was 2.44 \AA .

The second experiment was performed on the D10 single-crystal diffractometer at the Institut Laue-Langevin. This was operated in double-axis mode with a position-sensitive detector. A vertically curved pyrolytic graphite (002) monochromator was used in combination with a graphite filter. No collimators were used, but a circular aperture of diameter 6 mm was placed in the incident beam before the sample, and a square aperture of 12×12 mm was placed before the detector. The incident neutron wavelength was $2.356(4) \text{ \AA}$.

For both experiments we used a single crystal sample of PrO_2 which was prepared some time ago by a hydrothermal procedure⁷ and had a mass of ≈ 1 mg. For the first experiment the crystal was mounted inside a vertical-field superconducting cryomagnet with a temperature range of 2–300 K and a magnetic field range of 0–5 T. It was glued onto a thin aluminium pin such that the $[0\bar{1}1]$ direction was vertical and hence parallel to the applied field. For the second experiment the crystal was mounted inside a similar cryomagnet with a slightly larger field range of 0–6 T. It remained mounted on the aluminium pin, but was re-aligned using an attachment that held it at 45° so that the $[001]$ direction was vertical.

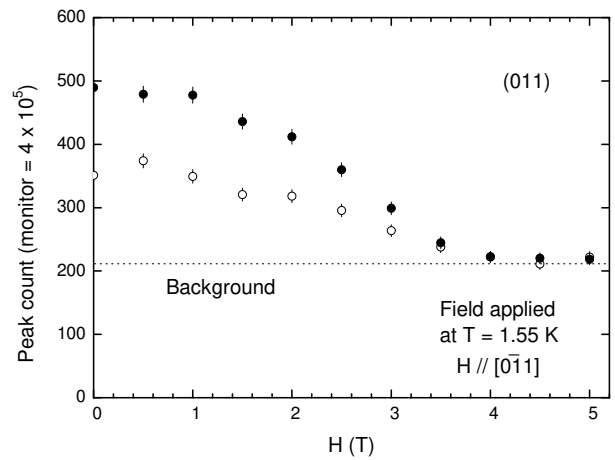


FIG. 2: Field dependence of the (011) magnetic Bragg reflection before (open circles) and after (closed circles) the irreversible increase in zero-field intensity. The field was applied parallel to $[0\bar{1}1]$ and the temperature was held constant at $T = 1.55 \text{ K}$ during both field sweeps.

B. Measurements with $H \parallel [0\bar{1}1]$

We first describe measurements performed on the E4 diffractometer. Five magnetic reflections of the type-I component of the magnetic structure were accessible in the horizontal scattering plane of the crystal ($[0\bar{1}1]$ vertical). These were (100), (011), (211), (122) and (300). At the start of the experiment the crystal was cooled to a temperature $T = 1.55 \text{ K}$ with zero applied field, and these five magnetic reflections plus several structural Bragg reflections were measured by crystal rotation (ω -scan).

After this we slowly increased the field from $H = 0 \text{ T}$ to $H = 5 \text{ T}$ in 0.5 T steps (while remaining at $T = 1.55 \text{ K}$) and monitored the count at peak centre of the (011) reflection. The intensity decreased continuously with field, reducing almost to zero at $H = 5 \text{ T}$. As we did not warm above T_N during the field sweep the disappearance of the (011) reflection suggested a spin reorientation transition rather than a change in the populations of the magnetic domains. To check that we could regain the original intensity, we immediately warmed the sample to $T = 20 \text{ K}$ under $H = 5 \text{ T}$, removed the field, cooled the sample back to $T = 1.55 \text{ K}$ in zero field, and re-measured the five type-I magnetic Bragg peaks. Surprisingly, the original intensities were not recovered. ω -scans revealed that the intensities of all five peaks had increased by $\sim 100\%$ relative to the initial zero-field measurement. The intensities of the (200) and (022) structural Bragg peaks were checked and found to be the same as they had been before application of the field. We then repeated the field scan from $H = 0 \text{ T}$ to $H = 5 \text{ T}$ at $T = 1.55 \text{ K}$ while counting at the centre of the (011) peak. The intensity was again found to reduce to zero (see Fig. 2). By monitoring the zero-field intensity of the (100) peak as a function of temperature, we determined that the Néel temperature had

not changed, remaining at $T_N = 13.5$ K.

To illustrate the increase in intensities of the five type-I magnetic Bragg peaks we compare in Fig. 3 the (100) and (011) peaks, measured in approximately zero field, before and after application and removal of the 5 T field associated with the above temperature cycling. We should mention that when the peaks were remeasured after the irreversible increase in intensities the magnetic field was actually set to $H = 0.5$ T, rather than $H = 0$ T, but subsequent field scans showed almost no difference between 0 T and 0.5 T (see Fig. 2).

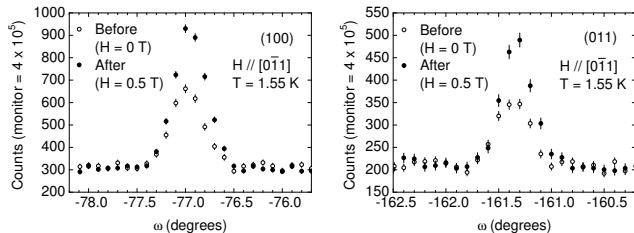


FIG. 3: ω -scans of the (100) and (011) magnetic Bragg reflections at $T = 1.55$ K, before (open circles) and after (closed circles) application and removal, above T_N , of a 5 T magnetic field parallel to the $[0\bar{1}1]$ direction. Detector counts are normalised to a fixed incident beam monitor count of 4×10^5 , corresponding to a counting time of ~ 4 minutes.

In an attempt to recover the original intensities of the five peaks the sample was heated to $T = 35$ K and cooled back down to 1.55 K in zero field. However, the original intensities were not recovered. The sample was then heated to $T = 123$ K and cooled back down in zero field. This time the original intensities were recovered.

As mentioned in the introduction, PrO_2 undergoes a structural distortion at $T_D = 120 \pm 2$ K, which is accompanied by an anomaly in the magnetic susceptibility.⁶ The fact that we were able to recover the original intensities of the magnetic Bragg reflections by heating to $T > T_D$ suggests that the PrO_2 ground state is metastable in the distorted phase. From now on we will refer to the Bragg intensities obtained by cooling through T_D in zero field as the “original intensities”.

The intensities of three of the reflections, (100), (011) and (211), were also measured by ω -scan at $H = 5$ T (after cooling through T_N in the 5 T field). The (100) and (211) reflections were found to have increased by $\sim 100\%$ from their original intensities at $H = 0$ T, whereas the (011) reflection was found to have decreased almost to the level of the background as reported above (see Fig. 2). The (100) and (011) peaks are shown in Fig. 4 for comparison with those shown in Fig. 3.

Since the (100) peak did not disappear at $H = 5$ T, we decided to check its field dependence. Starting from the original intensity, we found that when the field was applied at $T = 1.55$ K there was little change in intensity up to $H = 5$ T. However, when the crystal was warmed

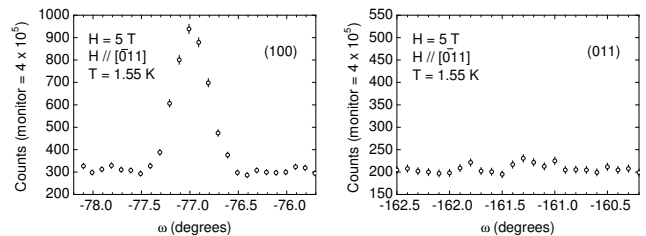


FIG. 4: ω -scans of the (100) and (011) magnetic Bragg reflections (normalised to a fixed incident beam monitor count), measured at $H = 5$ T after cooling through T_N in the field ($\mathbf{H} \parallel [0\bar{1}1]$).

above T_N and cooled to 1.55 K each time the field was incremented we observed a smooth increase in intensity with field. Furthermore, the increase did not become irreversible until the applied field was larger than $H = 3.5$ T. Once the 100% increase had been achieved, the intensity of the (100) reflection was unaffected by the applied field, whether the crystal was cooled through T_N in the field or not. The same was found to be true of the (211) and (300) reflections. However, the (122) reflection behaved more like the (011) reflection, decreasing to zero intensity at $H = 5$ T when cooled through T_N in the applied field.

The main findings from the measurements described so far with $\mathbf{H} \parallel [0\bar{1}1]$ are (i) the disappearance of certain magnetic Bragg reflections on application of a field $H \sim 5$ T, (ii) an irreversible 100% increase in intensity of all five peaks when the field is removed above T_N and the sample re-cooled to 1.55 K, (iii) recovery of the original intensities after heating above the structural distortion temperature $T_D = 120$ K and re-cooling in zero field. We also note that the irreversible increase in intensities can be generated by applying a field $H \sim 5$ T at 20 K, then cooling through T_N either before or after removing the field. The application of fields up to 5 T at $T = 1.55$ K does not cause the zero-field intensities to increase.

C. Measurements with $\mathbf{H} \parallel [001]$

The experiment performed on the D10 diffractometer was a repeat of the study performed on E4, but this time with the field applied parallel to the $[001]$ direction. Since the field was constrained to be vertical in both experiments the crystal orientation had to be changed for the D10 experiment. This altered the scattering plane and hence the range of accessible magnetic reflections. The type-I reflections accessible with our chosen neutron wavelength were (010), (110), (120), (030), (130) and (230). A number of half-integer reflections corresponding to the doubled component of the magnetic structure were also accessible, but only the $(\frac{1}{2}10)$ and $(\frac{3}{2}10)$ reflections had sufficient intensity to be measurable.

We measured these eight peaks by ω -scan at $T = 2.4$ K in zero applied field. We then warmed to 18 K, applied a field of 5.7 T, and re-cooled through T_N in the applied field. Before re-measuring the peaks we warmed to 18 K and removed the field before cooling back to $T = 2.4$ K (this second warming/cooling cycle was performed to reproduce the conditions under which the irreversible increase in intensities was first observed in the E4 experiment, i.e. field removed above T_N). The repeat ω -scans revealed that the (110) and (130) peaks reduced by $\sim 80\%$, while the other type-I peaks increased by $\sim 40\%$. The $(\frac{1}{2}10)$ and $(\frac{3}{2}10)$ peaks increased by $\sim 20\%$ and 30% respectively. Figure 5 shows the intensities of the (010) and (110) peaks before and after application and removal of the 5.7 T field associated with the above temperature cycling.

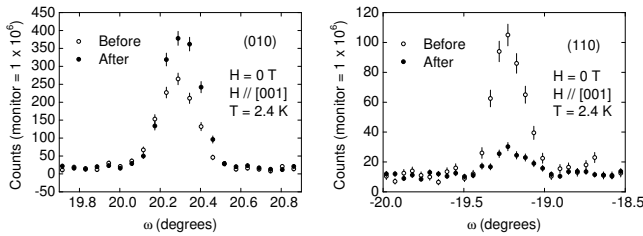


FIG. 5: The intensities of the (010) and (110) magnetic Bragg reflections at $T = 2.4$ K, measured at $H = 0$ T before (open circles) and after (closed circles) application and removal, above T_N , of a 5.7 T magnetic field parallel to the [001] direction. A monitor count of 1×10^6 corresponds to a counting time of ~ 2 minutes.

We then measured the (010), (110) and (230) peaks at $T = 2.4$ K, $H \geq 5$ T after cooling through T_N in the field. Their intensities remained approximately the same as those observed at zero field after application and removal of the 5.7 T field.

Figure 6 shows a plot of the count at peak centre for the (010) and (110) reflections as a function of applied field before and after the change in intensities. Each time the field was changed the crystal was warmed above T_N and cooled back to $T = 2.4$ K. Once the maximum field of 5.7 T had been applied, further changes in the applied field had little effect on the peak intensities.

In agreement with expectations following the E4 experiment, we found that application and removal of a large magnetic field (5.7 T) above T_N , followed by zero-field cooling caused an irreversible change in the intensities of the magnetic Bragg peaks. We also found that the original intensities could only be regained by heating the crystal to $T > T_D$ and re-cooling through T_D in zero field. The intensities of the (020) and (220) structural Bragg reflections were checked at $T = 2.4$ K, $H = 0$ T before and after application of the 5.7 T field. Again, these did not change. There was no change in the Néel temperature either, this remaining at $T_N = 13.4$ K for both integer and half-integer magnetic reflections.

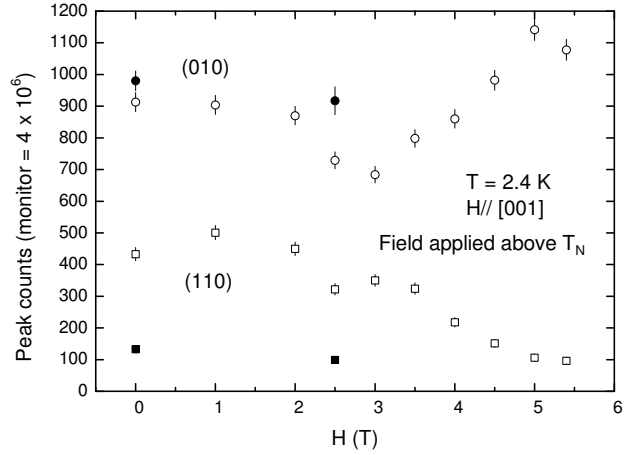


FIG. 6: Field dependence of the (010) and (110) magnetic Bragg reflections at peak centre before (open symbols) and after (closed symbols) the irreversible change in peak intensities. The magnetic field was applied parallel to the [001] direction, and the crystal was warmed above T_N and cooled back to $T = 2.4$ K each time the field was changed. Note that the monitor count for this data is four times that of the data displayed in Figure 5.

The most striking result from the measurements described above is that the changes in the peak intensities are different from those observed during the E4 experiment. In the E4 experiment (when H was applied along the $[0\bar{1}1]$ direction) all the peak intensities rose by $\sim 100\%$ after application and removal of a 5 T field, whereas in the D10 experiment (when H was applied along the [001] direction) the relative peak intensities changed: some peaks increased by $\sim 40\%$ while others decreased by $\sim 80\%$.

D. Data analysis

We obtained the integrated intensity of each magnetic Bragg reflection measured in the experiments described above by fitting a Gaussian profile to each peak, calculating its area and correcting for the geometrical Lorentz factor $L = \sin 2\theta$, where θ is the Bragg angle. Tables I and II list the integrated, corrected intensities and compare them with the square of the expected magnetic structure factor $\langle |F_M(\mathbf{Q})|^2 \rangle$ for a type-I antiferromagnetic structure under ambient conditions, i.e. where all the magnetic domains are equally populated. The magnetic structure factors were calculated using the formula

$$\langle |F_M(\mathbf{Q})|^2 \rangle = \sum_{\alpha\beta} \left\langle \left(\delta_{\alpha\beta} - \hat{Q}_\alpha \hat{Q}_\beta \right) F_M^\alpha(\mathbf{Q}) F_M^\beta(\mathbf{Q}) \right\rangle, \quad (1)$$

where the summation indices α and β run over the cartesian co-ordinates x, y and z , $\delta_{\alpha\beta}$ is the Kronecker delta,

\hat{Q}_α is the α -component of the unit scattering vector and $\langle \rangle$ denotes an average over all symmetry-equivalent magnetic domains. $F_M^\alpha(\mathbf{Q})$ is given by

$$F_M^\alpha(\mathbf{Q}) = f(\mathbf{Q}) \sum_j \hat{\mu}_j^\alpha e^{i\mathbf{Q} \cdot \mathbf{r}_j} e^{-W_j(Q,T)}, \quad (2)$$

where the summation index j runs over all the magnetic atoms in the magnetic unit cell, $\hat{\mu}_j^\alpha$ is the α -component of a unit vector in the direction of the magnetic moment of the j th magnetic atom, \mathbf{r}_j is the position of the j th magnetic atom within the magnetic unit cell, $f(\mathbf{Q})$ is the magnetic form factor of the Pr^{4+} ion and $e^{-W_j(Q,T)}$ is the Debye-Waller factor (we set this equal to 1, since the measurements were made at low temperatures).

The integrated intensities of the magnetic Bragg reflections are proportional to $\langle |F_M(\mathbf{Q})|^2 \rangle$ and the volume of the sample. For ease of comparison the intensities of the observed magnetic reflections listed in tables I and II have been normalised to the original intensity of the (100) reflection. Similarly, the $\langle |F_M(\mathbf{Q})|^2 \rangle$ have been normalised to the $\langle |F_M(\mathbf{Q})|^2 \rangle$ of the (100) reflection.

Reflection	$\mathbf{H} \parallel [0\bar{1}1]$			Domain-averaged $\langle F_{\text{M}}(\mathbf{Q}) ^2 \rangle$
	Before	After		
	$H = 0$	$H = 0.5 \text{ T}$	$H = 5 \text{ T}$	
(100)	1.00 ± 0.05	1.87 ± 0.05	1.93 ± 0.06	1.00
(011)	0.56 ± 0.04	1.00 ± 0.06	0.09 ± 0.05	0.48
(211)	0.63 ± 0.07	1.34 ± 0.09	1.18 ± 0.09	0.65
(122)	0.47 ± 0.07	0.91 ± 0.08	$*0.51 \pm 0.26$	0.38
(300)	0.56 ± 0.07	1.17 ± 0.09	$*1.67 \pm 0.31$	0.69

TABLE I: Comparison between integrated intensities of magnetic peaks (corrected for the Lorentz factor) before and after application of a 5 T magnetic field along $[0\bar{1}1]$. The intensities have been normalised to the original intensity of the (100) reflection. The $\langle |F_M(\mathbf{Q})|^2 \rangle$ have been normalised to the $\langle |F_M(\mathbf{Q})|^2 \rangle$ of the (100) reflection. The values marked with a * have been calculated from measurements of the count at peak centre, since no ω -scans were made at these positions.

For $\mathbf{H} \parallel [0\bar{1}1]$ the relative intensities of the magnetic Bragg reflections agree with the domain-averaged $\langle |F_M(\mathbf{Q})|^2 \rangle$ both before and after the irreversible increase in intensities. However, for $\mathbf{H} \parallel [001]$ the relative peak intensities only agree with the domain-averaged $\langle |F_M(\mathbf{Q})|^2 \rangle$ before the irreversible change.

E. Summary

To summarise the results of the neutron diffraction studies on single crystal PrO_2 , we have observed an irre-

Reflection	$\mathbf{H} \parallel [001]$			Domain-averaged $\langle F_{\text{M}}(\mathbf{Q}) ^2 \rangle$
	Before	After		
	$H = 0$	$H = 0$	$H \approx 5 \text{ T}$	
(010)	1.00 ± 0.09	1.43 ± 0.10	1.38 ± 0.10	1.00
(110)	0.50 ± 0.06	0.10 ± 0.03	0.09 ± 0.05	0.48
(120)	0.53 ± 0.11	0.76 ± 0.10		0.49
(030)	0.57 ± 0.08	0.79 ± 0.08		0.69
(130)	0.26 ± 0.06	0.07 ± 0.02		0.33
(230)	0.47 ± 0.07	0.65 ± 0.08	0.76 ± 0.16	0.49
$(\frac{1}{2}10)$	0.08 ± 0.02	0.10 ± 0.02		
$(\frac{3}{2}10)$	0.10 ± 0.02	0.13 ± 0.03		

TABLE II: Comparison between integrated intensities of magnetic peaks (corrected for the Lorentz factor) before and after application of a 5.7 T magnetic field along $[001]$. The intensities have been normalised to the original intensity of the (010) reflection. The $\langle |F_M(\mathbf{Q})|^2 \rangle$ have been normalised to the $\langle |F_M(\mathbf{Q})|^2 \rangle$ of the (010) reflection.

versible change in the magnetic Bragg intensities following the application and removal of a large magnetic field. The field required to induce this change is between 3.5 T and 5 T when $\mathbf{H} \parallel [0\bar{1}1]$ and $\leq 5.7 \text{ T}$ when $\mathbf{H} \parallel [001]$. To recover the original intensities the crystal must be heated to $T > T_D$ and re-cooled through T_D in zero field. The experimental results suggest that the field must be applied above T_N to induce the irreversible change in intensities. When the field is applied parallel to the $[0\bar{1}1]$ direction, certain peaks increase by $\sim 100\%$ while others disappear. After removal of the field, all peaks are found to have increased by $\sim 100\%$ relative to their original intensities. When the field is applied parallel to $[001]$ some of the type-I peaks increase by $\sim 40\%$ while others decrease by $\sim 80\%$. The half-integer peaks increase by 20–30%. These changes are preserved when the field is removed. The intensities of the structural Bragg reflections are unaffected by fields applied along either the $[0\bar{1}1]$ direction or the $[001]$ direction, and T_N remains unchanged.

III. INFLUENCE OF MAGNETIC FIELD ON DOMAIN POPULATIONS

We now attempt to interpret the observations summarised above by considering the possible influence of an applied magnetic field on the populations of structural and magnetic domains.

One of the original aims of the neutron diffraction experiments described above was to influence the popula-

tions of magnetic domains by cooling through T_N in a magnetic field. By applying the field along certain symmetry directions we hoped to break the symmetry of the crystal in such a way that certain domains would be energetically favoured. In the single- \mathbf{q} and double- \mathbf{q} magnetic structures some domains have zero magnetic structure factors. Therefore, altering the populations of the domains can alter the magnetic Bragg intensities. However, in the triple- \mathbf{q} structure all domains have identical magnetic structure factors, so in this case the Bragg intensities will be unaltered by changes in the domain populations.

The fact that we have observed changes in the intensities of the magnetic Bragg peaks after application of a magnetic field along two different symmetry directions rules out the triple- \mathbf{q} structure. We can also rule out the double- \mathbf{q} structure by calculating the single-domain magnetic structure factors for the observed reflections. We find no single domain whose squared magnetic structure factor is more than 50% larger than its value when averaged over all symmetry-equivalent domains. Thus the double- \mathbf{q} structure cannot account for the 100% increase in intensities observed when the field is applied along $[0\bar{1}1]$. However, to prove that the structure is single- \mathbf{q} and that the increase in intensities observed is due to preferential population of certain domains we must determine whether the increased intensities are consistent with the magnetic structure factors of the domains we expect to be favoured.

The single- \mathbf{q} transverse⁸ structure has six symmetry-equivalent domains, as the ordering wavevector can be along $[100]$, $[010]$ or $[001]$, and the spins can point along either of the two directions mutually perpendicular to the ordering vector. Tables III and IV show the single-domain $|F_M(\mathbf{Q})|^2$ calculated in these six domains for the magnetic Bragg peaks observed in the E4 and D10 experiments respectively. We use D_α^β to denote a domain with ordering vector along the α -direction and spins along the β -direction.

If we assume that the exchange interactions between the individual atomic spins are stronger than their interactions with the applied field, then for an antiferromagnetic structure we expect the domains with the lowest magnetic energy to be those whose spins lie perpendicular to the applied field. We therefore expect such domains to be favoured over those whose spins have components parallel and antiparallel to the field. If we use this assumption to predict which magnetic domains should be favoured in PrO_2 , we expect domains D_b^b and D_c^c to be favoured equally for $\mathbf{H} \parallel [0\bar{1}1]$. However, the magnetic structure factors in these domains are zero for all the peaks measured in the E4 experiment, in contradiction to the observed irreversible increase in intensities. Similarly, for $\mathbf{H} \parallel [001]$ we would expect domains D_a^b , D_b^a , D_c^a and D_a^c to be favoured equally. However, if we average the magnetic structure factors for these domains we find that they do not agree with the observed intensity changes.

Reflection	Single-domain $ F_M(\mathbf{Q}) ^2$						Domain-averaged $\langle F_M(\mathbf{Q}) ^2 \rangle$
	D_a^b	D_a^c	D_b^a	D_b^c	D_c^a	D_c^b	
(100)	3.00	3.00	0.00	0.00	0.00	0.00	1.00
(011)	1.42	1.42	0.00	0.00	0.00	0.00	0.48
(211)	1.96	1.96	0.00	0.00	0.00	0.00	0.65
(122)	1.14	1.14	0.00	0.00	0.00	0.00	0.38
(300)	2.06	2.06	0.00	0.00	0.00	0.00	0.69

TABLE III: Comparison between single-domain and domain-averaged $|F_M(\mathbf{Q})|^2$ for magnetic Bragg reflections observed in the E4 experiment (where the magnetic field was applied along $[0\bar{1}1]$). The single-domain $|F_M(\mathbf{Q})|^2$ have been normalised to the domain-averaged $\langle |F_M(\mathbf{Q})|^2 \rangle$ of the (100) reflection. D_α^β denotes a domain with ordering vector along the α -direction and spins along the β -direction.

Reflection	Single-domain $ F_M(\mathbf{Q}) ^2$						Domain-averaged $\langle F_M(\mathbf{Q}) ^2 \rangle$
	D_a^b	D_a^c	D_b^a	D_b^c	D_c^a	D_c^b	
(010)	0.00	0.00	3.00	3.00	0.00	0.00	1.00
(110)	0.00	0.00	0.00	0.00	1.42	1.42	0.48
(120)	0.49	2.46	0.00	0.00	0.00	0.00	0.49
(030)	0.00	0.00	2.06	2.06	0.00	0.00	0.69
(130)	0.00	0.00	0.00	0.00	1.77	0.20	0.33
(230)	0.00	0.00	1.20	1.74	0.00	0.00	0.49

TABLE IV: Comparison between single-domain and domain-averaged $|F_M(\mathbf{Q})|^2$ for magnetic Bragg reflections observed in the D10 experiment (where the magnetic field was applied along $[001]$). The single-domain $|F_M(\mathbf{Q})|^2$ have been normalised to the domain-averaged $\langle |F_M(\mathbf{Q})|^2 \rangle$ of the (010) reflection. D_α^β denotes a domain with ordering vector along the α -direction and spins along the β -direction.

The above observations suggest that our assumptions concerning the dominant spin interactions are incorrect. By inspection of table III we find better agreement between the structure factors and increased intensities if domains D_a^b and D_a^c are favoured for $\mathbf{H} \parallel [0\bar{1}1]$. Rather than having *spins* perpendicular to the applied field, these domains have *ordering vectors* perpendicular to the applied field. If these domains are favoured, the intensities of all the observed peaks should increase by a factor of 3. The observed increase is a factor of ~ 2 , but it is possible that this is due to incomplete depopulation of the disfavoured domains. Similarly, by inspection of table IV we find better agreement between the structure factors

and observed intensities if domains D_a^b , D_a^c , D_b^a and D_b^c are favoured for $\mathbf{H} \parallel [001]$. Again, these domains have ordering vectors (rather than spins) perpendicular to the applied field. If we average their squared magnetic structure factors we find that the (110) and (130) peaks are expected to disappear, while the rest are expected to increase by 50%. The observed decrease of the (110) and (130) intensities by $\sim 80\%$ and the increase of the other peaks by $\sim 40\%$ are consistent with a small portion of the crystal remaining populated with the disfavoured domains.

In the D10 experiment we also observed the $(\frac{1}{2}10)$ and $(\frac{3}{2}10)$ reflections to increase by 20–30% after application and removal of a large field parallel to $[001]$. These reflections arise from the doubled component of the magnetic structure.⁶ If we calculate the single-domain magnetic structure factors of the $(\frac{1}{2}10)$ and $(\frac{3}{2}10)$ reflections, we find that they are non-zero only in domains where the unit cell is doubled along the a -direction. Since the field was applied along $[001]$, i.e. the c -direction in the D10 experiment, we suggest that the applied field favours domains of the doubled component of the magnetic structure whose unit cells are doubled along the a - and b -directions, i.e. directions perpendicular to \mathbf{H} . The squared magnetic structure factors of the $(\frac{1}{2}10)$ and $(\frac{3}{2}10)$ reflections averaged over these domains are 50% larger than the structure factors averaged over all domains, in rough agreement with the observed increase in intensities of the peaks.

We have shown that magnetic domain alignment can account for the observed changes in magnetic Bragg intensities following application and removal of a large magnetic field. However, we have not yet discussed why the changes are irreversible below T_D . We propose that this is because certain domains of the distorted crystal structure are energetically preferred in an applied field. In other words, the application of a magnetic field at constant temperature below T_D causes a change in the structural domain population. Intuitively, it feels somewhat implausible that a 5 T magnetic field could cause a significant repopulation of structural domains at low temperatures. However, we must remember that the structural distortion is purely internal, so does not produce any macroscopic strain. All that is required is that the oxygen atoms move the small distance between equivalent shifted sites within the unit cell. Since it is likely that the cooperative Jahn-Teller distortion at T_D is accompanied by ordering of the Pr orbitals, we propose that the mechanism by which the field influences the structural domains is a coupling between the applied field and the Pr orbital magnetic moments. Our analysis indicates that the favoured structural domains are those whose unit cells are doubled along directions perpendicular to the applied field. The existence of a doubled component of the magnetic structure indicates a strong coupling between the lattice and the magnetic ordering, possibly via the Pr spin-orbit interaction. We therefore propose that the formation of magnetic domains on cooling through

T_N is influenced predominantly by the underlying alignment of the structural domains.

From our analysis of the favoured type-I magnetic domains it appears that coupling between the type-I component and the doubled component of the magnetic structure causes the ordering vector of the type-I component to lie parallel to the direction along which the unit cell is doubled. The strong influence of the structural domain alignment on the magnetic ordering of both the type-I component and the doubled component would account for the irreversibility of the changes in the magnetic Bragg intensities below T_D .

Finally we recall that in the E4 experiment the (011) and (122) reflections disappeared under the influence of a 5 T magnetic field along $[0\bar{1}1]$. This occurred both when the field was applied at constant $T = 1.55$ K and when the crystal was cooled through T_N in the field. The reflections reappeared when the field was removed. To explain these observations we propose that a reversible spin-reorientation transition occurs in the type-I component between $H = 0$ T and $H = 5$ T for $\mathbf{H} \parallel [0\bar{1}1]$. This causes the spins to rotate parallel and antiparallel to the field as shown in Fig. 7. We arrived at this spin configuration by trying various possibilities until we found one whose squared single-domain magnetic structure factors were in agreement with the relative intensities of the magnetic peaks observed at $H = 5$ T (see Table V). The configuration appears counterintuitive because an antiferromagnetic structure would normally minimise its energy by rotating its spins perpendicular to the field. However, our experimental results indicate a strong interaction between the lattice and the magnetism which could alter this simple picture.

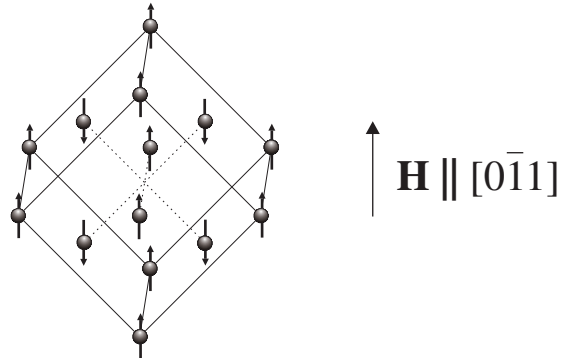


FIG. 7: Reorientated spin configuration of the type-I component of the magnetic structure at $H = 5$ T.

IV. SUSCEPTIBILITY MEASUREMENTS

We now present measurements of the magnetic susceptibility of single crystal PrO_2 . These measurements were made using a commercial SQUID magnetometer with a vertical field range of 0–7 T and a temperature range of

Reflection	Intensity at $H = 5$ T	Single-domain $ F_M(\mathbf{Q}) ^2$
(100)	1.93 ± 0.06	3.00
(011)	0.09 ± 0.05	0.00
(211)	1.18 ± 0.09	1.57
(122)	$*0.51 \pm 0.26$	0.23
(300)	$*1.67 \pm 0.31$	2.05

TABLE V: Comparison between integrated intensities of magnetic peaks (corrected for the Lorentz factor) measured under a field of 5 T parallel to [011] and single-domain $|F_M(\mathbf{Q})|^2$ for the structure shown in Fig. 7. The intensities have been normalised to the original intensity of the (100) reflection. The $|F_M(\mathbf{Q})|^2$ have been normalised to the domain-averaged $\langle |F_M(\mathbf{Q})|^2 \rangle$ of the (100) reflection for the type-I magnetic structure. The values marked with a * have been calculated from measurements of the count at peak centre, since no ω -scans were made at these positions.

2–300 K. The susceptibility was measured as a function of temperature and field, with the field applied along two different symmetry directions. The aim was to probe the bulk magnetisation of the crystal as a function of magnetic field to observe the effects of domain alignment and spin reorientation.

A. Experimental Details

We used two single crystals of PrO_2 for the susceptibility measurements. Both were taken from the same batch as the sample used in the neutron diffraction experiments, and each had a mass of < 1 mg. The crystals were mounted in plastic sample holders with the [110] and [001] directions vertical (hence parallel to the applied field). Their orientations were estimated to be accurate to within 5%. All measurements were made using the reciprocating sample option (RSO) which causes the sample holder to oscillate in the vertical direction.

B. Measurements and results

Here we present measurements of the magnetic susceptibility performed with the applied field parallel to the [110] and [001] directions. Results obtained for the two different field directions are compared and discussed.

It should be noted that the susceptibility measurements presented in this section are not normalized to the mass of the crystals because the crystals were too small to be weighed accurately. Hence, the susceptibility data taken in different field directions should not be compared quantitatively.

Figures 8(a) and 8(b) show the temperature dependence of the magnetic susceptibility in the range $T = 2$ –300 K when a field of $H = 1$ T is applied parallel to the [110] direction and when a field of $H = 0.3$ T is applied parallel to the [001] direction. Figures 8(c) and 8(d) show the same data as in Figs. 8(a) and 8(b) respectively, but depict the inverse susceptibility as a function of temperature, which makes the anomaly at $T_D = 120$ K more visible. The overall shape of the susceptibility trace is very similar for $\mathbf{H} \parallel [110]$ and $\mathbf{H} \parallel [001]$. However, the anomaly at T_D is more pronounced for $\mathbf{H} \parallel [110]$. This can be seen in the plots of both M/H vs T and $(M/H)^{-1}$ vs T .

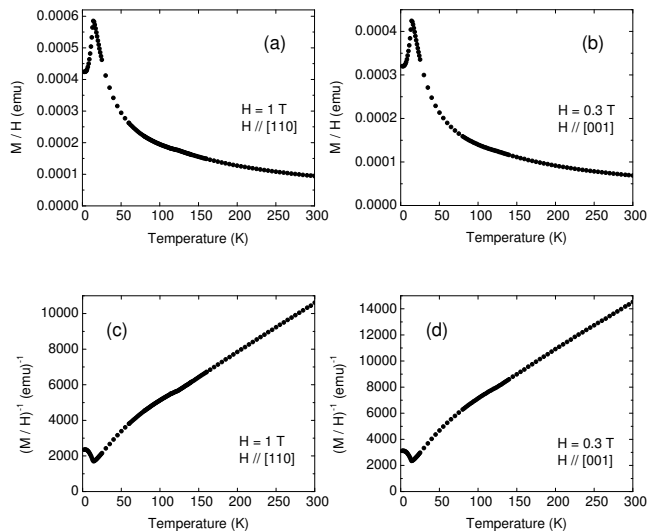


FIG. 8: Temperature dependence of the magnetic susceptibility of PrO_2 when the magnetic field is applied parallel to the [110] and [001] directions. Plots (c) and (d) show the inverse susceptibilities derived from the data in (a) and (b) respectively.

To investigate the field-dependence of the susceptibility, we made a series of measurements between 2 K and 20 K at different applied fields. The field was increased and decreased in steps from $H = 0$ T to $H = 7$ T. For each measurement we applied the field above T_N (at 20 K), then measured the susceptibility as a function of temperature while cooling through T_N . The data are shown in Fig. 9, with field increasing in 9(a) and 9(c) and decreasing in 9(b) and 9(d). For both field directions the susceptibility below T_N increases smoothly with field through the pale grey region (see 9(a) and 9(c)). Plots 9(c) and 9(d) are identical, showing that, for $\mathbf{H} \parallel [110]$ the increase below T_N is completely reversible and the susceptibility above T_N is independent of field. For $\mathbf{H} \parallel [001]$, a change occurs at $H = 1$ T. Below this field the susceptibility above T_N is independent of field, but above $H = 1$ T the whole trace increases irreversibly through the dark grey region shown in 9(a). When the field is removed,

the whole trace decreases through the smaller dark grey region shown in 9(b). As the field is decreased below $H = 1$ T the susceptibility above T_N becomes independent of field and the trace below T_N decreases through the pale grey region.

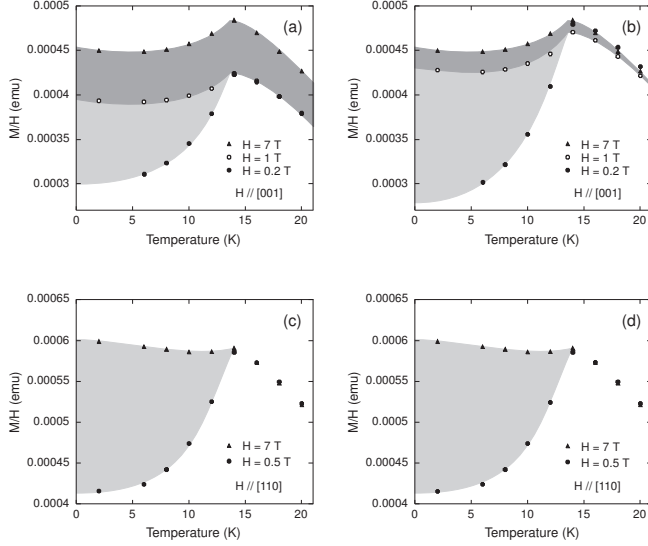


FIG. 9: Field-induced changes in the temperature-dependence of the susceptibility. The field is increased and decreased in steps, with each new field applied at $T = 20$ K. The susceptibility is measured as a function of T as the crystal is cooled through T_N . (a) and (b) show M/H for $\mathbf{H} \parallel [001]$. The field increases in (a) and decreases in (b). (c) and (d) show M/H for $\mathbf{H} \parallel [110]$. The field increases in (c) and decreases in (d).

It should be noted that repetitions of the susceptibility measurements at low applied fields revealed small, random shifts whenever the applied field was changed between measurements. This was attributed to fluctuations in the magnetisation of the sample surroundings and trapped flux in the superconducting magnet, leading to fluctuations in the applied field of 0.001–0.02 T. However, at higher fields the fluctuations became negligible compared to the total field, so the susceptibility was unaffected. Unfortunately it was impossible to measure the magnetisation of the sample surroundings, and it was therefore impossible to measure the exact applied field. This meant that the magnitude of the susceptibility at applied fields of $H \leq 0.2$ T had an uncertainty of at least $\pm 10\%$.

The plots in Fig. 10 are taken from the same data set as those in Fig. 9, but this time the susceptibility is plotted as a function of applied field instead of temperature. Figures 10(a) and 10(c) show the field dependence of the susceptibility below T_N , whereas Figs. 10(b) and 10(d) show the field dependence above T_N . For $\mathbf{H} \parallel [001]$ the susceptibility below T_N increases rapidly from $H = 0$ –1 T, then increases slowly and irreversibly from $H = 1$ –7 T (Fig. 10(a)). The susceptibility above T_N changes

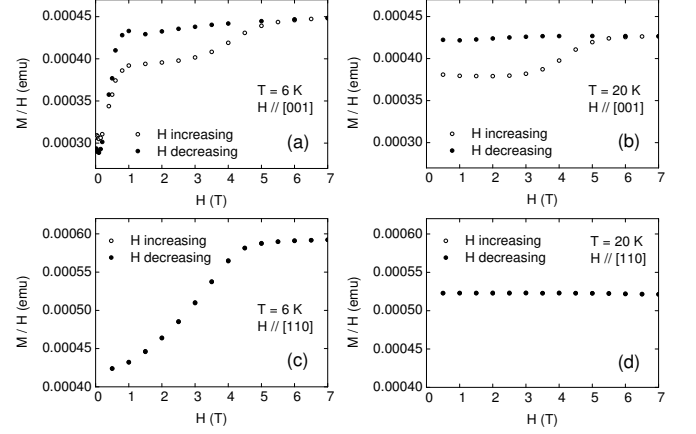


FIG. 10: Change in the field-dependence of the susceptibility with temperature. These plots are taken from the same data set as those in Fig. 9. Each time the applied field was changed, the crystal was warmed to $T = 20$ K, then cooled through T_N in the new applied field. (a) and (b) show M/H for $\mathbf{H} \parallel [001]$ below and above T_N respectively. (c) and (d) show M/H for $\mathbf{H} \parallel [110]$ below and above T_N .

little between $H = 0$ T and $H = 1$ T, but increases irreversibly between $H = 3$ T and $H = 7$ T (Fig. 10(b)). For $\mathbf{H} \parallel [110]$ the susceptibility below T_N increases rapidly and reversibly between $H = 0$ T and $H = 7$ T, but is almost independent of field above T_N .

In the measurements described above, the field was always applied above T_N . However, we also wished to investigate the field dependence of the susceptibility below T_N without cooling through T_N for each change in field. For this measurement the magnetic field was swept while keeping the temperature constant at 2 K. Figure 11 shows the results obtained. For $\mathbf{H} \parallel [110]$ the trace is very similar to that obtained when the crystal was cooled through T_N in the field. However, for $\mathbf{H} \parallel [001]$ there are two differences. Firstly, the irreversible increase occurs at a higher field. Secondly, on removal of the field at $T = 2$ K, the susceptibility does not return to its original zero field value. This contrasts with the data shown in Fig. 10(a), where removal of the field above T_N reduced the susceptibility below its original zero field value.

To see if an irreversible increase in the susceptibility occurred at higher temperatures we measured the field dependence at $T = 60$ K, with $\mathbf{H} \parallel [001]$. An irreversible increase did occur (see Fig. 12(a)), but of smaller magnitude than that observed at $T = 20$ K. To find the field required to make the increase irreversible, we warmed the crystal above T_D and re-cooled to $T = 60$ K in zero field. We then swept the field up and down several times, reaching successively larger values each time. We found that any increase in susceptibility, no matter how small, was irreversible (see Fig. 12(b)). For $\mathbf{H} \parallel [110]$ we found the susceptibility to be completely independent of field at $T = 60$ K. The data in Fig. 12(a) have been corrected

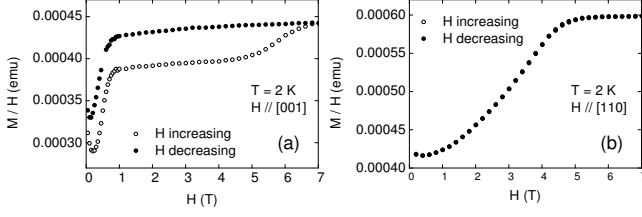


FIG. 11: Field-dependence of the susceptibility for field applied at constant $T = 2$ K. (a) $\mathbf{H} \parallel [001]$, (b) $\mathbf{H} \parallel [110]$. The small upturns in the susceptibility at low fields in both (a) and (b) are probably due to underestimation of the applied field strength, due to magnetisation of the sample surroundings.

for a remanent field of $H_R = 0.008$ T, which was probably caused by magnetisation of the sample surroundings or trapped flux in the superconducting magnet. H_R was determined by finding the y -intercept of a straight line fitted to a plot of magnetisation M versus field H ($M = \frac{M}{H}(H + H_R)$, where H_R is the remanent field).

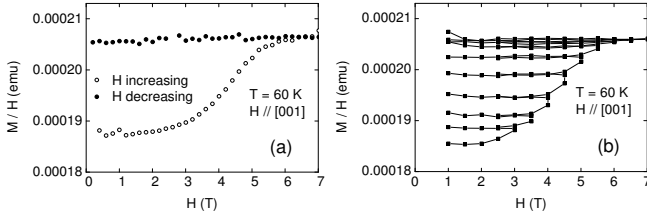


FIG. 12: Field-dependence of the susceptibility for $\mathbf{H} \parallel [001]$, field applied at constant $T = 60$ K. The data in (a) has been corrected for a small remanent field of $H_R = 0.008$ T, probably caused by magnetisation of the sample surroundings or trapped flux in the magnet. (b) shows that any increase in susceptibility, no matter how small, is irreversible.

The irreversible increase in susceptibility for $\mathbf{H} \parallel [001]$ persists up to T_D . This is shown in Fig. 13(a), where the temperature dependence of the susceptibility, measured at $H = 0.3$ T is plotted before and after application and removal of a 7 T field. The two traces coincide for $T > T_D$. Figure 13(b) shows the inverse susceptibility (taken from the same data set as Fig. 13(a)). The anomaly at T_D is more pronounced after application and removal of the 7 T field.

C. Summary

The main results of the susceptibility studies are as follows. The anomaly at T_D is more pronounced when the field is applied along $[110]$ than when it is applied along $[001]$. For $\mathbf{H} \parallel [110]$ the susceptibility increases reversibly with field below T_N , but is independent of field above

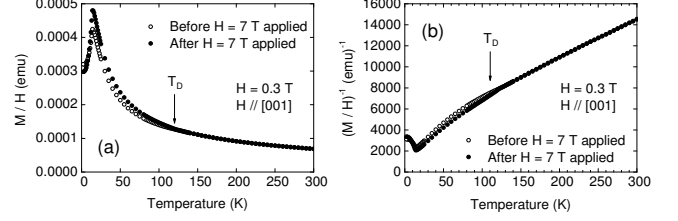


FIG. 13: Temperature-dependence of M/H at $H = 0.3$ T for $\mathbf{H} \parallel [001]$ before and after application and removal of a 7 T field. (a) M/H vs T . The two traces coincide above T_D . (b) $(M/H)^{-1}$ vs T . The anomaly at T_D is more pronounced after application and removal of the 7 T field.

T_N . For $\mathbf{H} \parallel [001]$ the susceptibility increases rapidly below T_N from $H = 0$ T to $H = 1$ T and more gradually from $H = 1$ T to $H = 7$ T. The increase from 0–1 T is quasi-reversible and occurs only below T_N , whereas the increase from 1–7 T is irreversible, and also occurs above T_N . The field strength at which the latter occurs depends on whether the field is applied below or above T_N . For fields applied at constant $T < T_N$ a field of 7 T is required to achieve the full increase in susceptibility, whereas for fields applied above T_N , only 5.5 T is required. Any increase in susceptibility above T_N , no matter how small, is irreversible. Above T_D the susceptibility is independent of field.

V. INTERPRETATION OF SUSCEPTIBILITY DATA

We now attempt to interpret the susceptibility data using our hypothesis that the formation of magnetic domains is strongly influenced by the distribution of structural domains.

The most likely cause of the reversible increase in susceptibility with field for $\mathbf{H} \parallel [110]$ is the proposed reversible spin reorientation in the type-I component of the magnetic structure.

For $\mathbf{H} \parallel [001]$ we propose that the rapid quasi-reversible increase in susceptibility between $H = 0$ T and $H = 1$ T is due to initial favouring of magnetic domains whose spins are perpendicular to the field (D_a^b , D_b^a , D_c^a and D_c^b). This would give rise to a small decrease in the magnetic structure factor of the (100) Bragg peak and a small increase in the magnetic structure factor of the (110) Bragg peak, in reasonable agreement with the small changes in Bragg intensities observed at $H = 1$ T (see Fig. 6). Between $H = 1$ T and $H = 7$ T we propose that the magnetic field becomes large enough to influence the alignment of the structural domains. The resulting structural domains cause those type-I magnetic domains whose ordering vectors are perpendicular to \mathbf{H} to be favoured. This leaves only domains D_a^b and D_b^a , causing the magnetic structure factors, and hence the in-

tensities of the Bragg reflections, to change. When the field is decreased below 1 T, we believe that domains D_a^c and D_b^c return. Combining the structure factors of these domains with those of D_a^b and D_b^a makes no difference to the average structure factors, in agreement with the observed absence of change in Bragg intensities on removal of the field. However, the return of these domains with spins parallel to the applied field would be expected to cause a decrease in susceptibility, as observed.

The above discussion shows that the hypotheses outlined in Section III provide some success in explaining the susceptibility data. However, some observations remain unexplained. For instance, we observe an irreversible increase in susceptibility between $H = 1$ T and $H = 7$ T for $\mathbf{H} \parallel [001]$ both below and above T_N . We assume that the increase above T_N is due to the effect of the applied field on the ordering of the Pr orbitals. However, no irreversible increase is observed either above or below T_N for $\mathbf{H} \parallel [110]$, and we do not understand why this should be. We also do not understand why a change in domain populations between $H = 0$ T and $H = 1$ T should cause a change in susceptibility for $\mathbf{H} \parallel [001]$ when the irreversible change in domain populations after application of a large field along $[110]$ causes no irreversible change in the susceptibility below T_N .

Despite the above problems, the interpretation of the susceptibility data is in broad agreement with that of the neutron diffraction data. We also note that the susceptibility measurements at low fields indicate that the $[001]$ direction is the easy direction of magnetisation, in support of a single- \mathbf{q} type-I component of the magnetic structure.

VI. CONCLUSION

We have presented (i) neutron diffraction studies of the antiferromagnetic structure of single crystal PrO_2 as a function of applied field (ii) susceptibility measurements

on single crystal PrO_2 as a function of applied field and temperature. Both studies were carried out for fields applied along two different symmetry directions: $[001]$ and $[110]$.

The neutron diffraction studies revealed irreversible changes in the magnetic Bragg intensities after application and removal of a large field. We attributed these changes to magnetic domain alignment, caused by a field-induced change in the underlying distribution of structural domains. For $\mathbf{H} \parallel [0\bar{1}1]$ we also observed certain reflections to disappear at high field and reappear when the field was removed. We attributed this observation to a spin reorientation of the type-I component of the magnetic structure.

The susceptibility studies revealed a reversible increase with applied field below T_N along both symmetry directions, as well as an irreversible increase at higher fields both above and below T_N for $\mathbf{H} \parallel [001]$. The irreversible increase disappeared at T_D , the temperature at which a cooperative Jahn-Teller distortion of the oxygen sublattice occurs. The changes in susceptibility with applied field are in broad agreement with the proposed alignment of structural and magnetic domains, although some features remain poorly understood.

We conclude that our neutron diffraction and susceptibility studies have revealed striking hysteresis effects on the application and removal of a large magnetic field below T_D . We propose that the field interacts strongly with the lattice to influence the alignment of structural domains below T_D , and that this in turn influences the alignment of the magnetic domains below T_N .

Acknowledgments

We would like to thank P. Santini for insightful discussions and F. Wondre for help with sample preparation. Financial support and provision of a studentship for CHG by the EPSRC is also acknowledged.

* Electronic address before May 1, 2004: carol.gardiner@npl.co.uk; Electronic address after May 1, 2004: carol.webster@npl.co.uk

¹ P. Santini, R. Lémanski, and P. Erdős, *Adv. Phys.* **48**, 537 (1999).

² J. A. Paixão, C. Detlefs, M. J. Longfields, R. Caciuffo, P. Santini, N. Bernhoeft, J. Rebizant, and G. H. Lander, *Phys. Rev. Lett.* **89**, 187202 (2002).

³ S. Kern, C.-K. Loong, J. Faber, Jr., and G. H. Lander, *Solid State Commun.* **49**, 295 (1984).

⁴ A. T. Boothroyd, C. H. Gardiner, S. J. S. Lister, P. Santini, B. D. Rainford, L. D. Noailles, D. B. Currie, R. S. Eccleston, and R. I. Bewley, *Phys. Rev. Lett.* **86**, 2082 (2001).

⁵ C. H. Gardiner, A. T. Boothroyd, S. J. S. Lister, M. J. McKelvy, S. Hull, and B. H. Larsen, *Appl. Phys. A* **74**, S1773 (2002).

⁶ C. H. Gardiner, A. T. Boothroyd, P. Pattison, M. J. McKelvy, G. J. McIntyre, and S. J. S. Lister, submitted to *Phys. Rev. B*.

⁷ M. McKelvy and L. Eyring, *J. Cryst. Growth* **62**, 635 (1983).

⁸ The longitudinal multi- \mathbf{q} structures are ruled out because they predict $\langle |F_M(\mathbf{Q})|^2 \rangle = 0$ for the (100) reflection, which is not observed either before or after application of a large magnetic field.